



Modeling of cancer-related body-wide effects identifies LTB₄ as a diagnostic biomarker for pancreatic cancer

Shu-Heng Jiang,^{a,1} Dejun Liu,^{b,1} Li-Peng Hu,^{a,1} Shan Zhang,^{a,1} Yanqiu Yu,^{c,d} Yong-Wei Sun,^{b,*} Jianguang Ji,^{e,*} and Zhi-Gang Zhang^{a,*}

^aState Key Laboratory of Oncogenes and Related Genes, Shanghai Cancer Institute, School of Medicine, Ren Ji Hospital, Shanghai Jiao Tong University, Shanghai 200240, PR China

^bDepartment of Biliary-Pancreatic Surgery, School of Medicine, Ren Ji Hospital, Shanghai Jiao Tong University, Shanghai 200217, PR China

^cDepartment of Pathophysiology, College of Basic Medical Sciences, China Medical University, Shenyang 110122, PR China

^dShenyang Engineering Technology R&D Center of Cell Therapy CO.LTD, Shenyang 110169, PR China

^eCenter for Primary Health Care Research, Lund University/Region Skåne, Sweden

Summary

Background Cancer elicits a complex adaptive response in an organism. Limited information is available for the body-wide effects induced by cancer. Here, we evaluated multiorgan changes in mouse models of pancreatic ductal adenocarcinoma (PDAC) and its precursor lesions (pancreatic intraepithelial neoplasia, PanIN) to decipher changes that occur during PDAC development.

Methods RNA-sequencing was employed in the brain, colon, stomach, kidney, heart, liver, and lung tissues of mice with PanIN and PDAC. A combination of differential expression analysis and functional-category enrichment was applied for an in-depth understanding of the multiorgan transcriptome. Differentially expressed genes were verified by quantitative real-time polymerase chain reaction. Neutrophil and macrophage infiltration in multiple organs was analyzed by immunohistochemical staining. Leukotriene B₄ (LTB₄) levels in mouse and human serum samples were determined by enzyme-linked immunosorbent assay.

Findings Transcriptional changes within diverse organs during PanIN and PDAC stages were identified. Using Gene Ontology enrichment analysis, increased neutrophil infiltration was discovered as a central and prominent affected feature, which occurred in the liver, lung, and stomach at the PanIN stage. The brain appeared to be well protected from the sequels of PanIN or PDAC. Importantly, serum LTB₄ was able to discriminate PDAC from normal controls, chronic pancreatitis, and intraductal papillary mucinous neoplasms with high performance.

Interpretation Our study provides a high-resolution cartographic view of the dynamic multiorgan transcriptomic landscape of mice with PDAC and its precursor lesions. Our findings suggest that LTB₄ could serve as a biomarker for the early detection of PDAC.

Funding The complete list of funders can be found in the Acknowledgement section.

Copyright © 2022 The Author(s). Published by Elsevier B.V. This is an open access article under the CC BY-NC-ND license (<http://creativecommons.org/licenses/by-nc-nd/4.0/>)

Keywords: Pancreatic cancer; Inter-organ communication; Systems biology; Systemic inflammation; Diagnostic marker

Abbreviations: PDAC, pancreatic ductal adenocarcinoma; PanIN, pancreatic intraepithelial neoplasia; LTB₄, leukotriene B₄; CP, chronic pancreatitis; IPMN, intraductal papillary mucinous neoplasms; ROC, receiver operating characteristics; DEG, differentially expressed gene; GO, gene ontology; CA19-9, carbohydrate antigen 19-9; NETs, neutrophil extracellular traps; PCA, principal component analysis

*Corresponding authors.

E-mail addresses: swyo616@126.com (Y.-W. Sun), jianguang.ji@med.lu.se (J. Ji), zzhang@shsci.org (Z.-G. Zhang).

¹ These authors contributed equally to this work.

eBioMedicine 2022;80:
104050
Published online xxx
<https://doi.org/10.1016/j.ebiom.2022.104050>

Research in context

Evidence before this study

Mounted studies in cancers focus on deciphering the changes that occur in primary tumors or metastatic lesions. Cancer-induced body-wide effects such as metabolic disorders and cachexia are commonly found at the late disease stage. Pancreatic ductal adenocarcinoma (PDAC) is often diagnosed too late for effective clinical treatment and lacks early diagnostics.

Added value of this study

This study conducted a characterization of the transcriptional differences of various distinct murine tissues (brain, colon, stomach, kidney, heart, liver, and lung) derived from mice with PDAC and its precursor lesions and provided baseline information regarding off-sites gene expression changes during PDAC development. Increased neutrophil infiltration in the liver, lung, and stomach was revealed to be an early event of PDAC. Neutrophil-derived LTB₄ could potentially be a PDAC biomarker since it was able to distinguish not only disease from controls but also chronic pancreatitis and intraductal papillary mucinous neoplasms.

Implications of all evidence available

This finding broadens our knowledge regarding the body-wide effects induced by PDAC and highlights the changes in neutrophilic inflammation during PDAC development. The results support the possibility of using LTB₄ as a serum biomarker for the early diagnosis of PDAC.

Introduction

Pancreatic ductal adenocarcinoma (PDAC), one of the most aggressive malignancies, is characterized by rapid progression, invasiveness, and refractoriness to most conventional therapies.¹ PDAC is the fourth leading cause of cancer-related deaths and is projected to be the second leading cause by 2030.² The majority of PDAC patients are usually diagnosed at an advanced stage with many facing distant organ metastases, rendering the option of curative resection unavailable and yielding a hopelessly dismal prognosis with a 5-year survival rate lower than 8%.³ In contrast, significantly better outcomes have been reported for small, early-stage, and surgically resectable PDAC. Therefore, identifying the changes at an early stage may improve early detection and provide effective therapeutic modalities for PDAC.

In investigating PDAC, accumulated studies deciphered changes that only occur in primary tumors or metastatic lesions.⁴⁻⁷ Nonetheless, the overarching view of cancer is a complicated, flexible, and systemic disease that encompasses whole-body-level disruptions, such as

insulin resistance, metabolic disorder, and cachexia.⁸⁻¹⁰ We know very little about the systemic interactions between cancer and host and the clinical significance of tumors on organismal physiology. Understanding the body's systemic responses to malignancy, especially at an earlier phase, may help with the early detection and cancer prevention of PDAC.¹¹

Tumor biomarkers refer to a class of substances that are synthesized and released not only by the tumor itself during tumor occurrence and development but also by the systemic response to cancer.¹² Thus, we reasoned that the body-wide changes in pancreatic carcinogenesis might provide effective biomarkers for early diagnosis and treatment of PDAC. Here, we profiled the global transcriptomic responses to PanIN and PDAC in seven mouse organs (liver, lung, colon, stomach, kidney, heart, and brain). Our findings showed that adaptive responses favor a succession of gene signatures used for neutrophilic inflammation. Furthermore, leukotriene B₄ (LTB₄), derived from neutrophils, was validated for the early detection of PDAC.

Methods

Mice

All mice used in this study were adult C57BL/6J and housed in specific pathogen-free conditions in the animal facility of the Shanghai Jiao Tong University. Mice were kept on a 12 h light-dark cycle at 23 ± 1 °C and a relative humidity range of 40–75%. All mice were fed with standard chow *ad libitum* and had access to water throughout the experiment. The conditional LSL-Kras^{G12D/+} mice, LSL-Trp53^{R172H/+} mice, and Pdx1-Cre mice were described previously.¹³ Genotype was confirmed by Southern blot analysis of mouse tail DNA according to the manufacturer's protocol (Bimake, B40013, Shanghai, China). At the endpoint of the experiment, mice were euthanized and the seven organs (liver, lung, colon, stomach, kidney, heart, and brain) were immediately isolated, snap-frozen in liquid nitrogen, and then stored at -80 °C. The entire procedure was conducted by three operators to expedite organ isolation and prevent RNA degradation. All mice were numbered and experiments were conducted in a blinded fashion. Age- and sex-matched littermates were used as controls in all the experiments. All mice used in this study had not undergone prior treatment or procedures.

RNA-sequencing analysis

Total RNA was extracted from the frozen organs with TRIzol reagent (TaKaRa, Kusatsu, Japan) followed by purification using an RNA 6000 Nano LabChip kit (Agilent Technologies, Palo Alto, CA, USA). The RNA quality

was inspected on a Bioanalyzer 2100 (NanoDrop, Agilent, Santa Clara, CA, USA). All tissue samples had clear bands of the 28 S and 18 S subunits of the ribosomal RNA, displayed no RNA degradation products and had an RNA integrity number (RIN) of ≥ 8 . The RNA-seq libraries were sequenced using Illumina HiSeq 2000 platform of Sinotech Genomics (Shenzhen, China). RNA-seq data processing, low-quality, and adapter-containing reads were trimmed by the Trim-galore software package. The trimmed sequences were aligned to mouse reference genome GRCm38/mm10 with HiSAT2 under default settings. The mapped reads of the genes that had the largest coefficients of variation based on the fragments were used for principal component analysis (PCA). The DESeq2 package was used to identify differentially expressed genes (DEGs) for all possible pairwise comparisons within each organ. Genes were considered differentially expressed if they had fold changes threshold at a level of 2 and $p < 0.05$. The DEGs from each organ were submitted to query for *Mus musculus* GO terms associated with biological processes by using the Database for Annotation, Visualization, and Integrated Discovery (DAVID, version 6.8). All RNA-seq data in this study have been deposited in the Sequence Read Archive (SRA) repository under accession number PRJNA715520.

Real-time quantitative PCR

Real-time qPCR was performed as previously reported.¹⁴ In brief, total RNA from the frozen tissues was extracted using TRIzol reagent (TaKaRa, Kusatsu, Japan) and reversely transcribed through a two-step PrimeScript RT-PCR kit (TaKaRa, Kusatsu, Japan) according to the manufacturer's instructions. Real-time qPCR analysis was done with SYBR-Green Premix Ex Taq (TaKaRa, Kusatsu, Japan) on a 7500 Real-time PCR system (Applied Biosystems, Foster City, USA). Relative mRNA expression was calculated based on the $2^{-\Delta\Delta Ct}$ method and normalized to β -actin mRNA levels. The primers used in this study were shown in **Supplementary Table 1**.

Immunohistochemical (IHC) staining

Hematoxylin and eosin (H&E) staining was performed routinely. IHC staining was performed as previously described.¹⁴ In brief, formalin-fixed paraffin-embedded (FFPE) sections (5 μ m) were routinely deparaffinized in xylene, rehydrated in a series of graded ethanol, followed by antigen retrieval with Tris/EDTA buffer (pH 9.0) and endogenous peroxidase blocking with 0.3% H₂O₂. Then, the sections were washed with Tris-buffered saline (pH 7.4) containing 0.05% Tween-20 (TBS-T) and blocked with TBS-T containing 5% goat serum (Sangon, Shanghai, China) for 1 h at room temperature. Next, sections were incubated with primary antibodies at 4 °C overnight. Detailed information for antibodies was shown as

follows: Ly6G (ab238132, diluted at 1:500, Abcam, Shanghai, China), CK19 (RRID:AB_2133325; 10712-I-AP, diluted at 1:1,000, Proteintech, Wuhan, China), and F4/80 (RRID:AB_2799771; #70076, diluted at 1:200, Cell Signaling Technology, Shanghai, China). The next day, tissue sections were incubated with a second antibody labeled with horseradish peroxidase-conjugated at room temperature for 1 h. Visualization of the target protein was performed by diaminobenzidine (DAB, GK3480, Gene Tech, Shanghai, China) and counterstained by hematoxylin. Negative controls had no primary antibodies applied. All the commercial antibodies have been validated. All the sections were observed and photographed with a microscope (Carl Zeiss, Oberkochen, Germany). Scoring was conducted independently by two senior pathologists in a blinded manner. The number of positive staining cells in each sample was counted in six random fields at 40 \times magnification, and the scores of the two experts were averaged as the final score for the sample. Two or three non-consecutive sections are evaluated as replicates.

Serum samples

The study population was comprised of 80 patients with histologically diagnosed PDAC, 36 patients with chronic pancreatitis (CP), 31 patients with intraductal papillary mucinous neoplasms (IPMN), and 96 healthy controls without a history of pancreatic diseases. The diagnoses of the patients with IPMN were guided by standard radiological imaging tests and determined by an experienced pancreatic expert. None of the enrolled patients (CP and IPMN) or healthy controls had a history of any tumors. Peripheral blood samples from PDAC patients with resectable tumors were collected obtained prior to any treatments (radiotherapy or chemotherapy) from Ren Ji Hospital, School of Medicine, Shanghai Jiao Tong University between July 1, 2018 and December 1, 2020, and were annotated with detailed information regarding age, sex, diagnosis, disease stage, and histology. For healthy controls, an equal distribution between males and females was sought and individuals aged over 60 are preferably included; inclusion criteria for healthy individuals were: normal blood pressure, normal body mass index (> 20 and < 30), normal physical activity level, no chronic conditions, no psychiatric disorder, and no alcohol intake. Healthy controls were selected from the same population that the patients came from and were recruited from the outpatient physical examination population, thus representing the healthy population in the study region, hospital, and setting. Blood samples were coagulated at room temperature for 30 min and centrifuged at 2000 g for 15 min, and the obtained serum was aliquoted, and then stored at -80 °C and shipped on dry ice.

Mouse blood samples were obtained from cohorts of LSL-Kras^{G12D/+}; Pdx-1-Cre (KC) and LSL-Kras^{G12D/+}; LSL-

Trp53^{R172H/+}; Pdx-1-Cre (KPC) mice and their littermate controls by accessing the retroorbital plexus. Blood was collected into micro-centrifuge tubes, allowed to clot at room temperature for 45 min, and serum supernatant was acquired by centrifugation (2000 g × 15 min) and stored at -80 °C.

LTB4 and CA19-9 measurement

LTB4 levels in serum samples were determined by a commercial enzyme-linked immunosorbent assay (ELISA) kit according to the manufacturer's instructions (KGE006B, R&D Systems, Minnesota, USA). The concentrations of LTB4 were obtained from standard curves of positive control proteins from the kits with a four-parameter logistic regression model. When the concentration of LTB4 was less than 15.6 pg/mL (the lowest limit of the standard curve), the value was set as equal to zero. Serum levels of CA19-9 were determined by chemiluminescence immunoassay with an Abbott-Architect immunoanalyzer (Abbott Laboratories, Abbott Park, IL, USA). Assays for serum LTB4 and CA19-9 were done by two researchers who are blinded to each subject.

Ethics

The human studies were reviewed and approved by the Research Ethics Committee of Ren Ji Hospital, School of Medicine, Shanghai Jiao Tong University (approval number RA-2021-095), and were in accordance with the principle of the Helsinki Declaration (No. KY2016-75). Written informed consent was obtained from all participants and the use of each sample collection was approved by the local institutional review boards. All mice were maintained and handled following the recommendation of the Guidelines for the Care and Use of Laboratory Animals published by the National Institutes of Health (NIH Publications No. 8023, revised 1978). The animal studies were reviewed and approved by the Research Ethics Committee of Ren Ji Hospital, School of Medicine, Shanghai Jiao Tong University (approval number 20191204).

Role of funders

The funders had no role in study design, data collection, data analyses, data interpretation, or writing of the report.

Statistical analysis

Data were presented as the means ± SD if not indicated. All experiments were performed on biological replicates unless otherwise specified. Statistical analysis for each experiment was performed using GraphPad Prism 7 software (La Jolla, CA, USA). Unpaired two-tailed independent samples t-test and the paired

t-test were used to estimate statistically significant differences between the two groups, respectively. One-way analysis of variance (ANOVA) followed by two-tailed post hoc Tukey's multiple comparison test was used for multiple comparisons. Receiver operating characteristics (ROC) curves were constructed to determine sensitivity, specificity, and respective areas under the curves (AUCs) with 95% confidence intervals. $P < 0.05$ was considered statistically significant.

Results

Summary of multiorgan transcriptomic profiling

The advent of high-throughput multiomics tremendously facilitates the elucidation of the recurrent genetic alterations underlying PDAC development and progression. Mutational activation of the *KRAS* gene is found in nearly all PDAC cases.^{15–17} In mice, oncogenic *Kras*^{G12D} mutations induce acinar-to-ductal metaplasia, pancreatic intraepithelial neoplasia (PanIN), and ultimately invasive PDAC.¹⁸ The addition of known mutations in tumor suppressors such as *TP53*, *SMAD4*, and *CDKN2A* accelerates the progression of these PanIN lesions and results in the rapid generation of invasive and metastatic malignancies.¹⁹ These mouse models faithfully recapitulate the genetic and biological evolution of human PDAC. To investigate global gene expression dynamics and to identify tissue-specific and tissue-enriched regulators associated with early pancreatic carcinogenesis and the development of PDAC, we generated a preclinical mouse model of PDAC and its noninvasive neoplastic precursor lesion PanIN (Figure 1a). To detect changes induced by very early precursor disease, a younger cohort of KC mice, with average age 6 months ($n = 6$), was used (hereafter designated as early phase disease). The well-established KPC mouse model was used to generate spontaneously arising pancreatic tumors (hereafter designated late-phase disease). KPC mice with distant metastases, such as liver and lung metastases, were excluded from the analysis. Three KPC mice ($n = 3$) aged 121, 174, and 146 days (an average age of 20 weeks) were included for investigation, and to mitigate disparities, their age- and sex-matched littermates [LSL-*Kras*^{G12D/+} or LSL-*Kras*^{G12D/+}; LSL-Trp53^{R172H/+} (KP)] served as controls (Supplementary Table 2). KC and KPC mice displayed no conspicuous histological changes in six tissues (liver, lung, colon, stomach, kidney, and brain) compared with their normal counterparts except for the heart, which presents typical vacuolar degeneration in both KC and KPC mice (Supplementary Fig. 1). H&E staining and CK-19 expression confirmed the ductal phenotype of PanIN and PDAC tissues (Figure 1b). RNA sequencing (RNA-seq)-based expression profiling was performed to analyze the transcriptome of seven organs dissected

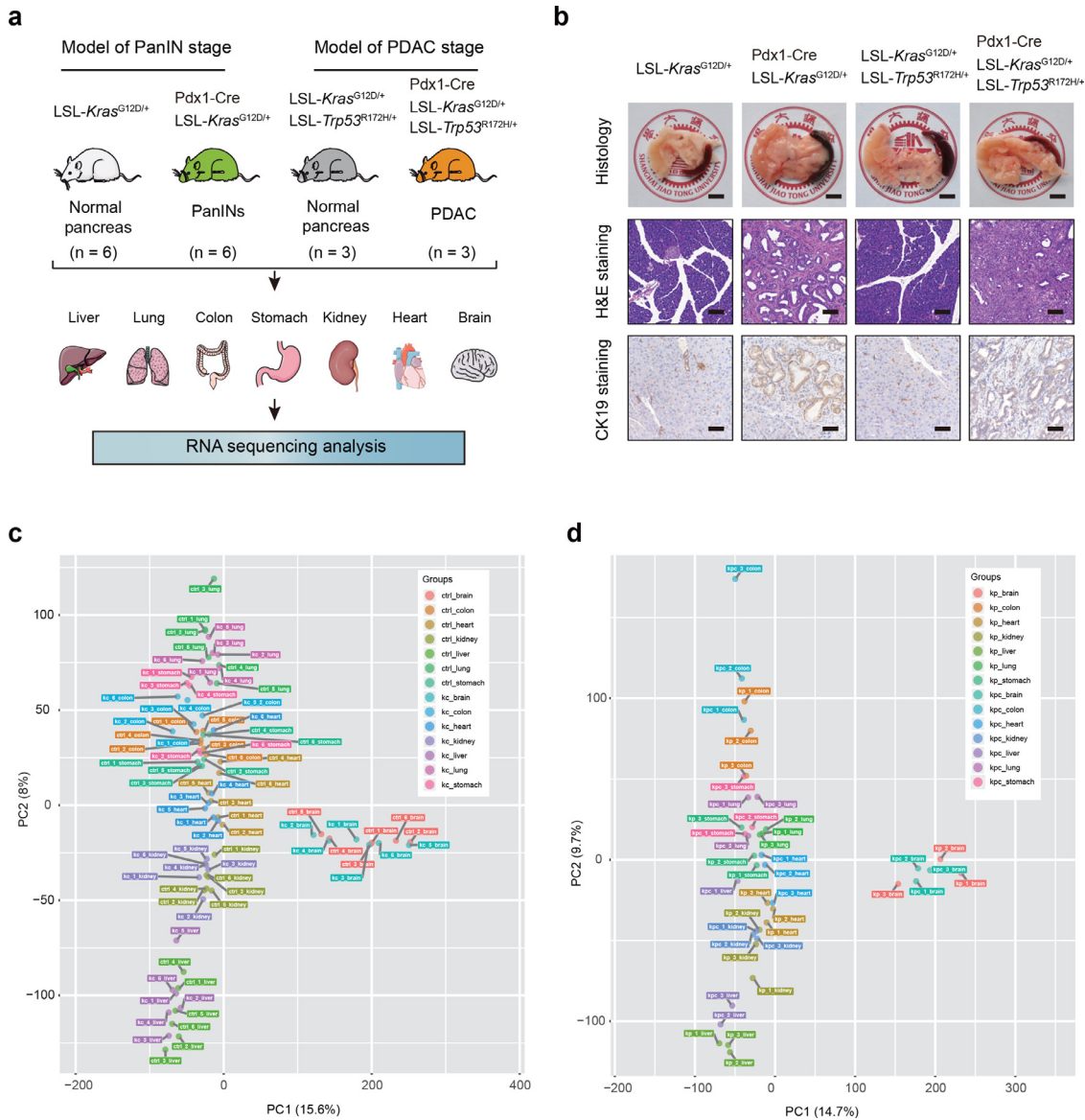


Figure 1. Summary of multi-organ transcriptomic profiling. **(a)** Schematic diagram of the experimental design for early and late phases of pancreatic disease; Pdx1-Cre; LSL-Kras^{G12D/+} (KC; n = 6) mice with an average age of 6 months were used to generate an early phase disease model, while Pdx1-Cre; LSL-Kras^{G12D/+}; LSL-Trp53^{R172H/+} (KPC; n = 3) mice were used to generate spontaneously arising pancreatic tumors (late-phase disease). **(b)** Gross photograph, H&E staining, and IHC for the epithelial marker CK19 of pancreata from KC and KPC mice and their respective control animals; scale bar: 0.5 cm for histology image and 50 μ m for H&E staining and IHC analysis. **(c, d)** Principal component analysis (PCA) plots for early-phase and late-phase samples, respectively; each dot represents the gene expression profile of an organ (indicated by different colors); the data indicates inherent variations in gene expression between biological samples.

from the mice mentioned above. Next, we conducted PCA to illustrate relationships between all samples based on the covariance of the data being examined. As a result, PCA revealed that there were varying degrees of differences between tissues, such as the stomach, lung and colon, which were less different, while the liver and brain were significantly different from other

tissues and organs. PCA performed on each organ yielded no significant separation during the PanIN stage (Figure 1c). Of note, there was a striking separation between KP and KPC samples, especially the liver, colon, lung, and stomach, suggesting that a dichotomy of gene expression profiles of these organs is likely induced by PDAC (Figure 1d).

revealed the magnitude of organ response during the early PanIN phase and the additive effect of the later PDAC periods. As shown in [Figure 2c](#), most DEGs were organ specific. Thus, we pursued the universal effects of PanINs and PDAC on gene expression in diverse organs. This analysis yielded multiple sets of known and newly identified genes affected by PanIN and PDAC, respectively. For instance, we found increased expression levels of *Capg*, *Akr1c18*, and *Lgals3* in the liver, colon, and stomach tissues; increased expression levels of *Csf3r* in the liver, lung, and stomach tissues; and decreased expression of atypical chemokine receptor 3 (*Ackr3*), a decoy and scavenger receptor for inflammatory CC chemokines,²⁰ in the lung and colon tissues ([Figure 2c](#)). Among DEGs affected by PDAC, plasminogen activator, urokinase receptor (*Plaur*), tropomyosin 3, related sequence 7 (*Tpm3-rs7*), a cellular marker for neutrophils (*Cd177*),²¹ and the innate immunity protein Tag7 (*Pglyrp1*),²² were consistently upregulated in all detected organs except for the brain. In contrast, the expression of the heat shock protein *Hspa1a* gene was substantially repressed in four of the seven organs ([Figure 2d](#)). Additionally, tumor-bearing KPC mice had remarkably higher expression of neutrophil-associated genes (*S100a8* and *S100a9*) and several inflammatory genes (*Chil3*, *Il1b*, *Ccl2*, *Retnlg*, and *Trim30a*) than KC mice in most organs except for the stomach ([Figure 2e](#), [Supplementary Fig. 3](#), and [Supplementary Tables 17–23](#)). These findings were further confirmed by real-time qPCR analysis ([Supplementary Fig. 4](#)). Taken together, the global transcriptomic profile unearthed by our systems biology-based approach mirrors the distinct disease stage of PDAC.

Neutrophilic inflammation induced by PanINs and PDAC

To better appreciate the putative biological relevance of the hundreds of DEGs identified, we performed functional-category enrichment analyses to produce a comprehensive overview of the canonical processes in PanIN and PDAC. The biological pathway analysis returned considerable results for the liver, lung, stomach, and colon but not for the kidney, heart, and brain at the early stage; clearly, the most prominent changes that occurred in the liver, lung, and stomach were leukocyte chemotaxis, granulocyte chemotaxis, neutrophil migration, and neutrophil chemotaxis, which emerged as the main affected features of particular interest ([Figure 3a-c](#)); in contrast, colon tissues showed evidence of altered regulation of energy homeostasis ([Figure 3d](#)). Neutrophils have been deemed the most abundant innate immune effector cells and are known to play a central role in multiple oncogenic processes, from initiation to seeding at distant organs.^{23,24} We quantified the infiltration of neutrophils by IHC staining for the neutrophil marker lymphocyte antigen 6G (Ly6G).

Importantly, Ly6G⁺ cells accumulated in the liver, lung, and stomach but not in other organs of KC mice ([Figure 3e](#)). At the late stage, Gene Ontology (GO) enrichment analyses revealed a clear dominance of inflammatory neutrophil accumulation in the liver, kidney, and heart tissues ([Supplementary Fig. 5](#)), suggesting that neutrophils not only accumulate in organs where metastases were primarily detected but also in the rarely metastatic organs. Different from observations from KC mice, histological analysis showed that neutrophil infiltration was not increased in lung and stomach tissues of KPC mice ([Figure 3f](#)). Therefore, organ-specific and stage-dependent neutrophilic inflammation implies that neutrophils undergo dynamic changes during PDAC development. Additionally, DEGs in the lung tissues at the late stage were enriched in defense response to fungus and cholesterol esterification, whereas in the colon and stomach, changes in gene expression of keratinization and regulation of endocytosis were prominent, respectively ([Supplementary Fig. 5](#)). Of note, the brain was not affected during the entire disease period. Accumulated evidence suggests that macrophages overshadow the roles of neutrophils in cancer.^{25,26} Indeed, the number of F4/80⁺ macrophages was markedly increased in the liver, lung, and stomach of KPC but not KC mice ([Supplementary Fig. 6](#)). Therefore, neutrophilic inflammation instead of other inflammatory responses induced by PanINs is a very early indicator for PDAC development.

Leukotriene B4 is an early diagnostic biomarker for PDAC

Serum-based protein biomarker screening could greatly improve PDAC patient survival in appropriately selected high-risk individuals, such as patients with a family history, hereditary pancreatitis, Peutz-Jeghers syndrome, and new-onset diabetes mellitus.²⁷ Here, we aimed to identify PDAC serum biomarkers based on the principle of cancer-related body-wide effects. Considering the crucial role of neutrophils implicated in the early phase of PDAC development, we investigated the possibility of neutrophil-secreted factors as potential biomarkers to facilitate the early detection of PDAC. Leukotriene B4 (LTB4) is a major product of arachidonic acid metabolism and has been implicated as known mediator of allergic and inflammatory diseases.²⁸ Previously, neutrophil-derived leukotrienes, including LTB4, were revealed to support lung colonization by selectively expanding cancer cells with high tumorigenic potential.²⁹ Therefore, we wondered whether serum LTB4 distinguishes KPC-afflicted animals from normal animals. To address this issue, we collected 20 PDAC serum samples from KPC mice and 20 samples from their littermate controls. ELISA results showed that LTB4 levels in PDAC samples were 2-fold higher than those in normal controls ([Figure 4a](#)). Comparing PDAC

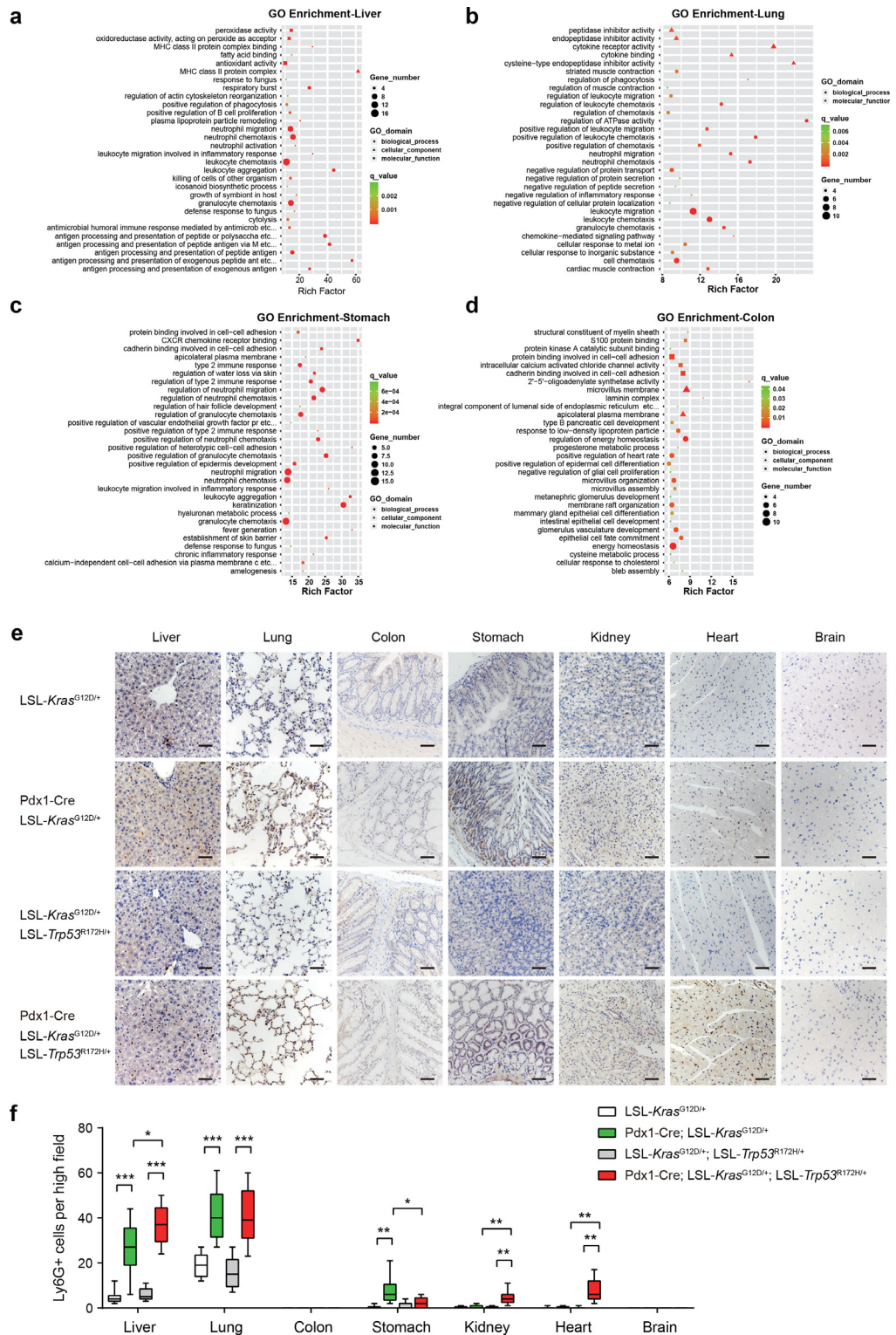


Figure 3. Neutrophilic inflammation induced by PanINs and PDAC. (a-d) Gene Ontology (GO) enrichment analysis of DEGs from the early phase disease in indicated organs; liver (a), lung (b), stomach (c), and colon (d). **(e)** IHC for Ly6G of seven organs from KC and KPC mice and their respective control animals; scale bar: 50 μ m. **(f)** Statistical analysis of Ly6G⁺ neutrophil infiltration in tissues from (e); the box represents the 25–75th percentiles, and the median is indicated; P values are derived from the ANOVA followed by post hoc Tukey's multiple comparison test. * $p < 0.05$; ** $p < 0.01$; *** $p < 0.001$.

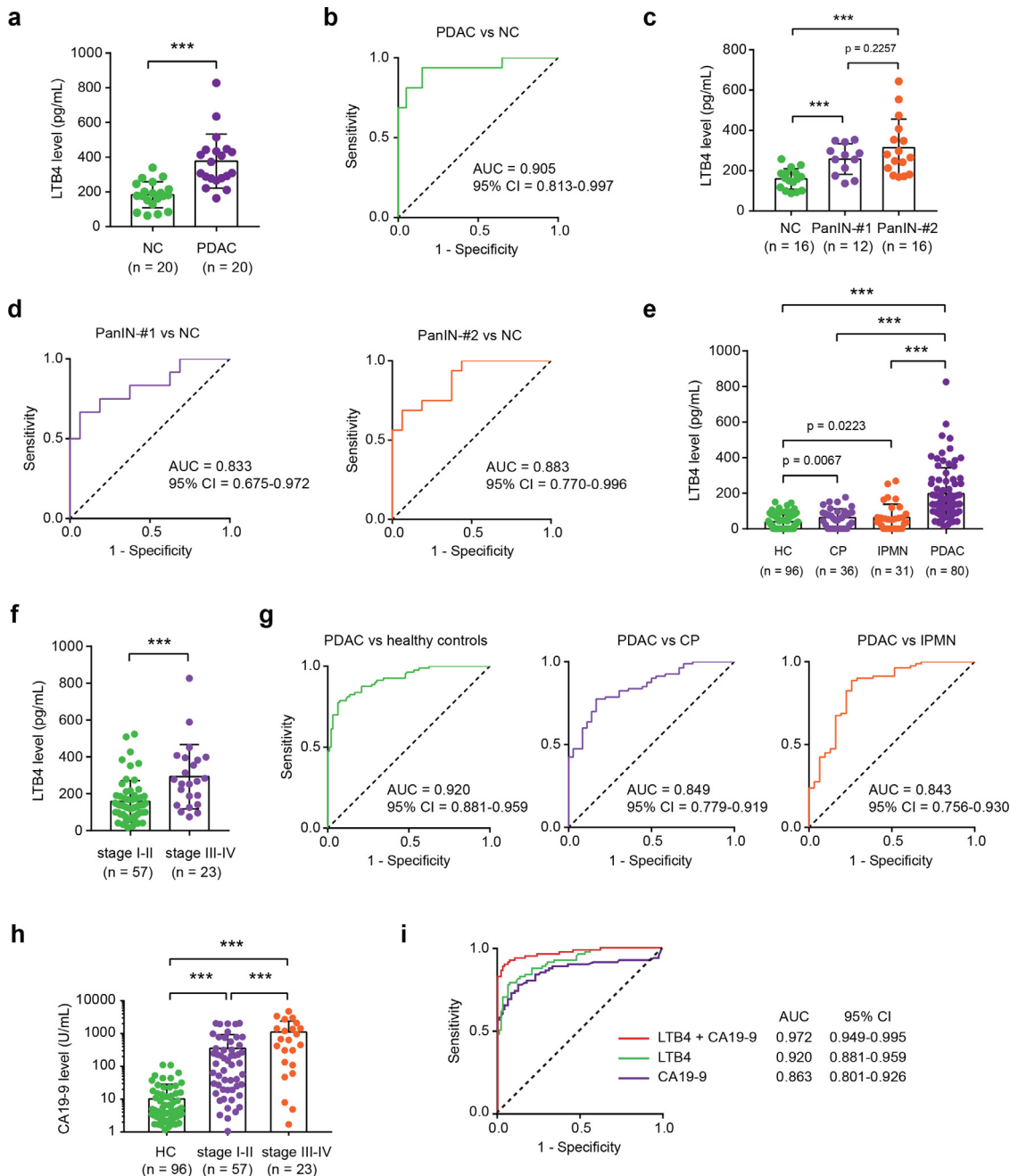


Figure 4. LTB4 is an early diagnosis marker for PDAC. **(a)** LTB4 concentrations in the serum from KPC mice ($n = 20$) and normal control animals ($n = 20$); P value is derived using the paired t-test statistics. **(b)** ROC curve for LTB4 in mice with PDAC versus normal controls. **(c)** LTB4 concentrations in the serum from KC mice at two PanIN cohorts; PanIN #1 mice have an average age of 5.5 ± 0.5 months ($n = 12$) and PanIN #2 mice have an average age of 9.0 ± 0.5 months ($n = 16$); P values are derived from the ANOVA followed by post hoc Tukey's multiple comparison test. **(d)** ROC curve for LTB4 in mice with PanIN versus normal controls. **(e)** LTB4 concentrations in the serum from human PDAC ($n = 80$), chronic pancreatitis ($n = 36$), intraductal papillary mucinous neoplasms (IPMN, $n = 31$), and healthy controls (HC, $n = 96$); P values are derived from the ANOVA followed by post hoc Tukey's multiple comparison test. **(f)** LTB4 concentrations in the serum from stage I-II ($n = 57$) and stage III-IV PDAC ($n = 23$); P value is derived using the independent samples t-test statistics. **(g)** ROC curve for LTB4 in all patients with PDAC versus healthy controls, CP, and IPMN. **(h)** CA19-9 concentrations in the serum from healthy controls ($n = 96$), stage I-II PDAC ($n = 57$) and stage III-IV PDAC ($n = 23$); P values are derived from the ANOVA followed by post hoc Tukey's multiple comparison test. **(i)** ROC curve for LTB4, CA19-9, and combination of both in PDAC patients versus healthy controls. * $p < 0.05$; ** $p < 0.01$; *** $p < 0.001$.

and normal controls gave an area under the receiver operating characteristic (ROC) curve (AUC) of 0.905 (95% CI, 0.813 to 0.997) (Figure 4b).

Having established the potential feasibility of LTB₄ in detecting invasive PDAC in mice, we next endeavored to perform a study on early phase disease. For this purpose, we used two cohorts of PanIN mice, a younger cohort of animals with an average age of 5.5 ± 0.5 months (PanIN #1) and an older cohort of animals with an average age of 9.0 ± 0.5 months (PanIN #2), which have relatively low and high burdens of PanIN, respectively (Supplementary Fig. 7). The median ELISA value for LTB₄ in the two PanIN cohorts was higher than that observed in normal controls (Figure 4c). When considering PanIN cases versus normal controls, c-statistics for LTB₄ increased from 0.833 (95% CI, 0.675 to 0.972) to 0.883 (95% CI, 0.770 to 0.996) with the PanIN #1 and PanIN #2 data, respectively (Figure 4d). Thus, these results suggest that LTB₄ can detect even very early pre-invasive disease.

To assess the clinical relevance of the described findings, we compared serum LTB₄ and CA19-9 levels in 243 participants: 80 with PDAC, 36 with chronic pancreatitis (CP), 31 with IPMN, and 96 healthy participants. The demographic characteristics of the study population are presented in Supplementary Table 24. The serum level of LTB₄ in PDAC was significantly higher than that in the other three groups; compared with healthy controls, a slight increase in the serum LTB₄ concentration in patients with chronic pancreatitis and IPMN was also observed (Figure 4e). Patients with stage III-IV PDAC had significantly higher LTB₄ concentrations than patients with stage I-II PDAC (Figure 4f). To investigate whether LTB₄ could distinguish PDAC from healthy controls and benign pancreatic diseases, we performed logistic regression to estimate its discriminatory ability. As a result, the PDAC cohorts could be discerned with a c-statistic value of 0.920 (95% CI, 0.881 to 0.959); LTB₄ was able to discriminate PDAC cases versus chronic pancreatitis with a c-statistic of 0.849 (95% CI, 0.779 to 0.919); again, PDAC versus IPMN could be differentiated with a c-statistic value of 0.843 (95% CI, 0.756 to 0.930) (Figure 4g). Thus, LTB₄ appeared to distinguish patients with PDAC from those with nonmalignant pancreatic diseases and healthy controls. Carbohydrate antigen 19-9 (CA19-9) is a useful diagnostic biomarker for PDAC management.²⁷ Consistent with a previous report,³⁰ CA19-9 was increased with advancing tumor stage (Figure 4h). In our cohort, CA19-9 alone achieved an AUC of 0.863 (95% CI, 0.801 to 0.926), which is less than that of LTB₄; if LTB₄ was combined, the AUC increased significantly, reaching 0.972 (95% CI, 0.949 to 0.995) (Figure 4i). Collectively, these results suggest that LTB₄ has the potential to distinguish PDAC patients from healthy controls.

Discussion

Cancer produces a variety of collateral tissue damage in patients beyond the tumor itself.⁸ The goal of this study was to identify the molecular changes in multiple organs induced by PDAC and its precursor lesions. To this end, we provided a comprehensive resource on the global mRNA expression changes during PanIN and PDAC. We recapitulated several reported molecular effects while providing additional insights into tumor-driven systemic perturbations. Additionally, we presented the possibility of using of LTB₄ for early detection of PDAC.

A growing body of evidence indicates that tumors can manipulate neutrophils to create diverse functional polarization states able to sustain tumor growth, suppress T-cell activation, induce angiogenesis, and facilitate tumor metastasis or occurrence.²³⁻³¹ In PDAC, inhibition of neutrophil recruitment by blocking CXCR2 suppresses metastases and augments immunotherapy.³² Consistent with this notion, the neutrophil-to-lymphocyte ratio (NLR), which reflects the cancer-induced systemic inflammatory response, has been proposed as an attractive factor for the risk stratification of cancer patients. An increase in neutrophil level or NLR may suggest tumor recurrence or progression, and a decrease in NLR after initiation of therapy may predict a good response.¹ The NLR is an independent predictive marker of IPMN-associated invasive malignancy.³³ As a complementary finding to these theories, we provided evidence that neutrophil infiltration in multiple organs is induced at an early disease stage of PDAC. The consequence of infiltrating neutrophils in these organs without tumor cells at this stage is not clear. The lung and liver are the most common metastatic sites for PDAC, and the accumulation of neutrophils in these tissues of KC mice may suggest the role of neutrophils in the pre-metastatic niche at a very early time. Indeed, neutrophils use various mechanisms, such as neutrophil extracellular traps (NETs), to shape the premetastatic niche for the subsequent implantation of cancer cells at this site.^{34,35} In line with our findings, Coffelt et al. revealed that neutrophil depletion reduces breast cancer lung metastasis in the early phase, but not the late stage, indicating that neutrophils promote tumor metastasis during the early steps of the metastatic cascade.³⁶ In cancer-associated cachexia, catabolic changes in cardiac muscle are induced by multiple proinflammatory cytokines arising from crosstalk between cancer cells and the immune system.⁸ In this study, whether the vacuolar degeneration of cardiomyocytes observed in KC and KPC mice is associated with neutrophil-derived factors and related to cancer-associated cachexia remains an active area of study. In addition, the biological significance of neutrophil accumulation in other nonmetastatic tissues is also worthy of further investigation. Considering this, targeting neutrophils may provide an

opportunity to counteract several of the tumor-induced systemic pathologies. How do neutrophils accumulate in these organs? Previously, cancer cell-intrinsic p53 was demonstrated to induce the secretion of WNT ligands that promote tumor-associated macrophages to produce IL-1 β , which further drives systemic neutrophilic inflammation in breast cancer.³⁷ Consistently, adipocyte-secreted IL1 β facilitates the recruitment of tumor-associated neutrophils in pancreatic cancer.³⁸ Given the high prevalence of Kras mutation in the early phase of PDAC, whether neutrophil accumulation is induced by a Kras-dependent mechanism remains an open question.

Our study may have clinical implications. The identification of reliable serum biomarkers is of paramount importance to the diagnosis of cancer, especially for the detection and screening of early-stage cancer.³⁹ LTB₄ is a lipid byproduct of arachidonate 5-lipoxygenase (ALOX5) that is secreted by chemotactic neutrophils, forming a secondary gradient in response to primary chemoattractants.^{40–42} Serum LTB₄ concentrations are widely reported to be higher in patients with bronchial asthma and allergic rhinitis than in healthy subjects.²⁸ In cancers, several reports have documented the critical roles of LTB₄ during tumor initiation and metastasis. For instance, reducing LTB₄ biosynthesis by inhibiting ALOX5 with Zileuton suppresses breast cancer pulmonary metastasis.^{29,43} Similarly, deletion of the key enzymes in LTB₄ biosynthesis, ALOX5 or LTA4H, significantly abrogated Kras-driven tumorigenesis or tumor burden in a xenograft mouse model.^{44,45} Here we identified LTB₄ as a biomarker for the detection of precursor lesions of PDAC in mice. In clinical settings, LTB₄ can distinguish PDAC from healthy individuals with satisfactory sensitivity and specificity compared with CA19-9. Consistently, LTB₄ levels remained unchanged in the pancreas in a rat model of chronic pancreatitis.⁴⁶ Although our data suggest the possibility of neutrophil-derived LTB₄, we cannot fully rule out the inputs of LTB₄ derived from other cells. Indeed, mast cells secrete LTB₄ to orchestrate a tumor-promoting neutrophilic inflammatory loop,⁴⁷ vascular smooth muscle cells can produce LTB₄ in response to HCMV-induced pathogenesis in inflammatory diseases,⁴⁸ and adipocytes generate LTB₄ to induce obesity-associated inflammation and insulin resistance in mice.⁴⁹

In this study, serum LTB₄ level was associated with an advanced disease stage in PDAC patients, suggesting possible therapeutic approaches against LTB₄ for PDAC treatment. Targeting of LTB₄ can be achieved by pharmacological intervention of its biosynthesis. Recently, the ALOX5 inhibitor has emerged as a therapeutic agent for cancer in several experimental models.⁵⁰ Notably, the specific ALOX5 inhibitor zileuton is widely used for the prophylaxis and treatment of chronic asthma. Zileuton blocks LTB₄ production and reduces spontaneous lung metastasis in MMTV-PyMT

tumor-bearing mice without altering primary tumors or lung neutrophil levels.²⁹ Moreover, Alox5 blockade with zileuton abrogates JAK2V617F-stimulated cell growth.⁵¹ These data suggest that repurposing zileuton usage could be a safer therapeutic option for PDAC treatment.

There are several limitations to our study. First, the RNA of the pancreatic tissue of two control groups was severely degraded due to the action of pancreatic digestive enzymes, and could not be used for sequencing analysis. Therefore, it is hard to deduce the common pathways between primary tumor/PanIN lesions and other vital organs. Secondly, only one cohort was used to investigate the diagnostic value of LTB₄ in pancreatic cancer. In the future, it will be interesting to launch a large-scale, multicenter investigation with a test cohort and an independent validation cohort that is encouraged to ascertain the clinical diagnostic relevance of LTB₄ as a serum biomarker for PDAC alone or in combination with CA19-9. Thirdly, the molecular mechanism underlying the link between pancreatic cancer/PanIN lesions and neutrophil-derived LTB₄ is not known. Further works are needed to elucidate how primary pancreatic lesions affect distant vital organs.

This study demonstrates the body-wide transcriptome landscape of two disease stages of PDAC. These results provide insight into the identification of candidate molecular changes for the detection of early-stage PDAC, especially LTB₄. Moreover, our findings reveal that PDAC mortality can be reduced by LTRAs, offering hope for new therapeutic strategies and treatments of PDAC. Thus, our work has important implications for understanding how cancer affects host physiology and ultimately blocking the pathological changes caused by the tumor for a better quality of life for PDAC patients.

Contributors

S-HJ, D-JL, L-PH, and SZ carried out *in vivo* experiments, manuscript preparation, and statistical analysis; S-HJ and SZ contributed to bioinformatics analysis; S-HJ, D-JL, and L-PH provided clinical specimens and made clinical pathology evaluations; S-HJ and SZ performed IHC analysis; S-HJ and D-JL contributed to ELISA experiment; Y-QY provided critical review; Y-WS, J-GJ and Z-GZ conceived, designed, supervised, analyzed and interpreted the study and provided critical review. S-HJ and Z-GZ have verified the underlying data. All authors read and approved the final version of the manuscript.

Data sharing statement

All RNAseq data has been deposited in Sequence Read Archive (SRA) repository under accession number PRJNA71520. Summary data are available in the paper and in supplementary materials. Raw data that support

the findings of this study are available from the corresponding author upon request.

Declaration of interests

The authors declare that they have no competing interests.

Acknowledgments

We thank technical help from Department of Pathology, Ren Ji Hospital, School of Medicine, Shanghai Jiao Tong University. The research was supported by grants from National Natural Science Foundation of China (82173153 and 81902370 to S-HJ); 92168111 to Z-GZ), Shanghai Municipal Education Commission-Gaofeng Clinical Medicine Grant Support (20181708 to Z-GZ), Program of Shanghai Academic/Technology Research Leader (19XD1403400 to Z-GZ), Shanghai Sailing Program (19YF1445700 to S-HJ), and Shanghai Chengguang Program (19CG17 to S-HJ), Medicine and Engineering Interdisciplinary Research Fund of Shanghai Jiao Tong University (YG2021ZDo8), Innovative research team of high-level local universities in Shanghai.

Supplementary materials

Supplementary material associated with this article can be found in the online version at doi:10.1016/j.ebiom.2022.104050.

References

- Mizrahi JD, Surana R, Valle JW, Shroff RT. Pancreatic cancer. *Lancet*. 2020;395(10242):2008–2020.
- Rahib L, Smith BD, Aizenberg R, Rosenzweig AB, Fleshman JM, Matrisian LM. Projecting cancer incidence and deaths to 2030: the unexpected burden of thyroid, liver, and pancreas cancers in the United States. *Cancer Res*. 2014;74(11):2913–2921.
- Huang J, Lok V, Ngai CH, et al. Worldwide burden of, risk factors for, and trends in pancreatic cancer. *Gastroenterology*. 2021;160(3):744–754.
- Renz BW, Takahashi R, Tanaka T, et al. β_2 adrenergic-neurotrophin feedforward loop promotes pancreatic cancer. *Cancer Cell*. 2018;33(1):75–90.e7.
- Ruscetti M, Morris JP, Mezzadra R, et al. Senescence-induced vascular remodeling creates therapeutic vulnerabilities in pancreas cancer. *Cell*. 2020;181(2):424–441.e21.
- Chung KM, Singh J, Lawres L, et al. Endocrine-exocrine signaling drives obesity-associated pancreatic ductal adenocarcinoma. *Cell*. 2020;181(4):832–847.e18.
- Lee JW, Stone ML, Porrett PM, et al. Hepatocytes direct the formation of a pro-metastatic niche in the liver. *Nature*. 2019;567(7747):249–252.
- Baracos VE, Martin L, Korc M, Guttridge DC, Fearon KCH. Cancer-associated cachexia. *Nat Rev Dis Prim*. 2018;4:17105.
- Jiang SH, Zhang XX, Hu LP, et al. Systemic regulation of cancer development by neuro-endocrine-immune signaling network at multiple levels. *Front Cell Dev Biol*. 2020;8: 586757.
- Masri S, Papagiannakopoulos T, Kinouchi K, et al. Lung adenocarcinoma distally rewires hepatic circadian homeostasis. *Cell*. 2016;165(4):896–909.
- Kozawa S, Ueda R, Urayama K, et al. The body-wide transcriptome landscape of disease models. *iScience*. 2018;2:238–268.
- Brand RE, Nolen BM, Zeh HJ, et al. Serum biomarker panels for the detection of pancreatic cancer. *Clin Cancer Res*. 2011;17(4):805–816.
- Jiang SH, Li J, Dong FY, et al. Increased serotonin signaling contributes to the warburg effect in pancreatic tumor cells under metabolic stress and promotes growth of pancreatic tumors in mice. *Gastroenterology*. 2017;153(1):277–291.e19.
- Jiang SH, Zhu LL, Zhang M, et al. GABRP regulates chemokine signalling, macrophage recruitment and tumour progression in pancreatic cancer through tuning KCNN4-mediated Ca^{2+} signalling in a GABA-independent manner. *Gut*. 2019;68(11):1994–2006.
- Cancer Genome Atlas Research Network. Cancer genome atlas research network. Integrated genomic characterization of pancreatic ductal adenocarcinoma. *Cancer Cell*. 2017;32(2):185–203.e13.
- Biankin AV, Waddell N, Kassahn KS, et al. Pancreatic cancer genomes reveal aberrations in axon guidance pathway genes. *Nature*. 2012;491(7424):399–405.
- Waddell N, Pajic M, Patch AM, et al. Whole genomes redefine the mutational landscape of pancreatic cancer. *Nature*. 2015;518(7540):495–501.
- Hingorani SR, Petricoin EF, Maitra A, et al. Preinvasive and invasive ductal pancreatic cancer and its early detection in the mouse. *Cancer Cell*. 2003;4(6):437–450.
- Mazur PK, Sivek JT. Genetically engineered mouse models of pancreatic cancer: unravelling tumour biology and progressing translational oncology. *Gut*. 2012;61(10):1488–1500.
- Meyrath M, Szpakowska M, Zeiner J, et al. The atypical chemokine receptor ACKR3/CXCR7 is a broad-spectrum scavenger for opioid peptides. *Nat Commun*. 2020;11(1):3033.
- Zhou G, Yu L, Fang L, et al. CD177+ neutrophils as functionally activated neutrophils negatively regulate IBD. *Gut*. 2018;67(6):1052–1063.
- Yashin DV, Ivanova OK, Soshnikova NV, et al. Tag7 (PGLYRP1) in complex with Hsp70 induces alternative cytotoxic processes in tumor cells via TNFR1 receptor. *J Biol Chem*. 2015;290(35):21724–21731.
- Jaillon S, Ponzetta A, Di Mitri D, Santoni A, Bonecchi R, Mantovani A. Neutrophil diversity and plasticity in tumour progression and therapy. *Nat Rev Cancer*. 2020;20(9):485–503.
- Albregues J, Shields MA, Ng D, et al. Neutrophil extracellular traps produced during inflammation awaken dormant cancer cells in mice. *Science*. 2018;361(6409):ea04227.
- DeNardo DG, Ruffell B. Macrophages as regulators of tumour immunity and immunotherapy. *Nat Rev Immunol*. 2019;19(6):369–382.
- Ng LG, Ostuni R, Hidalgo A. Heterogeneity of neutrophils. *Nat Rev Immunol*. 2019;19(4):255–265.
- Pereira SP, Oldfield L, Ney A, et al. Early detection of pancreatic cancer. *Lancet Gastroenterol Hepatol*. 2020;5(7):698–710.
- Yokomizo T, Nakamura M, Shimizu T. Leukotriene receptors as potential therapeutic targets. *J Clin Invest*. 2018;128(7):2691–2701.
- Wculek SK, Malanchi I. Neutrophils support lung colonization of metastasis-initiating breast cancer cells. *Nature*. 2015;528(7582):413–417.
- Kim J, Bamlet WR, Oberg AL, et al. Detection of early pancreatic ductal adenocarcinoma with thrombospondin-2 and CA19-9 blood markers. *Sci Transl Med*. 2017;9(398):eaah5583.
- Coffelt SB, Wellenstein MD, de Visser KE. Neutrophils in cancer: neutral no more. *Nat Rev Cancer*. 2016;16(7):431–446.
- Steele CW, Karim SA, Leach JDG, et al. CXCR2 inhibition profoundly suppresses metastases and augments immunotherapy in pancreatic ductal adenocarcinoma. *Cancer Cell*. 2016;29(6):832–845.
- Gemenetzis G, Bagante F, Griffin JF, et al. Neutrophil-to-lymphocyte ratio is a predictive marker for invasive malignancy in intra-ductal papillary mucinous neoplasms of the pancreas. *Ann Surg*. 2017;266(2):339–345.
- Lee W, Ko SY, Mohamed MS, Kenny HA, Lengyel E, Naora H. Neutrophils facilitate ovarian cancer premetastatic niche formation in the omentum. *J Exp Med*. 2019;216(1):176–194.
- Yang L, Liu Q, Zhang X, et al. DNA of neutrophil extracellular traps promotes cancer metastasis via CCDC25. *Nature*. 2020;583(7814):133–138.

- 36 Coffelt SB, Kersten K, Doornebal CW, et al. IL-17-producing $\gamma\delta$ T cells and neutrophils conspire to promote breast cancer metastasis. *Nature*. 2015;522(7556):345–348.
- 37 Wellenstein MD, Coffelt SB, Duits DEM, et al. Loss of p53 triggers WNT-dependent systemic inflammation to drive breast cancer metastasis. *Nature*. 2019;572(7770):538–542.
- 38 Incio J, Liu H, Suboj P, et al. Obesity-induced inflammation and desmoplasia promote pancreatic cancer progression and resistance to chemotherapy. *Cancer Discov*. 2016;6(8):852–869.
- 39 Singhi AD, Koay EJ, Chari ST, Maitra A. Early detection of pancreatic cancer: opportunities and challenges. *Gastroenterology*. 2019;156(7):2024–2040.
- 40 Gelfand EW. Importance of the leukotriene B₄-BLT₁ and LTB₄-BLT₂ pathways in asthma. *Semin Immunol*. 2017;33:44–51.
- 41 Miyabe Y, Miyabe C, Luster AD. LTB₄ and BLT₁ in inflammatory arthritis. *Semin Immunol*. 2017;33:52–57.
- 42 Bhatt L, Roinestad K, Van T, Springman EB. Recent advances in clinical development of leukotriene B₄ pathway drugs. *Semin Immunol*. 2017;33:65–73.
- 43 Tang L, Wang Z, Mu Q, et al. Targeting neutrophils for enhanced cancer therapeutics. *Adv Mater*. 2020;32(33) e2002739.
- 44 Knab LM, Schultz M, Principe DR, et al. Ablation of 5-lipoxygenase mitigates pancreatic lesion development. *J Surg Res*. 2015;194(2):481–487.
- 45 Oi N, Jeong CH, Nadas J, et al. Resveratrol, a red wine polyphenol, suppresses pancreatic cancer by inhibiting leukotriene A₄hydro-lase. *Cancer Res*. 2010;70(23):9755–9764.
- 46 Zhou W, Levine BA, Olson MS. Lipid mediator production in acute and chronic pancreatitis in the rat. *J Surg Res*. 1994;56(1):37–44.
- 47 Jala VR, Bodduluri SR, Satpathy SR, Chheda Z, Sharma RK, Hari-babu B. The yin and yang of leukotriene B₄ mediated inflammation in cancer. *Semin Immunol*. 2017;33:58–64.
- 48 Qiu H, Strååt K, Rahbar A, Wan M, Söderberg-Nauclér C, Haeggström JZ. Human CMV infection induces 5-lipoxygenase expression and leukotriene B₄ production in vascular smooth muscle cells. *J Exp Med*. 2008;205(1):19–24.
- 49 Mothe-Satney I, Filloux C, Amghar H, et al. Adipocytes secrete leukotrienes: contribution to obesity-associated inflammation and insulin resistance in mice. *Diabetes*. 2012;61(9):2311–2319.
- 50 Du F, Yuelling L, Lee EH, et al. Leukotriene synthesis is critical for medulloblastoma progression. *Clin Cancer Res*. 2019;25(21):6475–6486.
- 51 Chen Y, Shan Y, Lu M, et al. Alox₅ blockade eradicates JAK2V617F-induced polycythemia vera in mice. *Cancer Res*. 2017;77(1):164–174.